Regulatory B cell production of IL-10 inhibits lymphoma depletion during CD20 immunotherapy in mice

Mayuka Horikawa, Veronique Minard-Colin, Takashi Matsushita, and Thomas F. Tedder

Department of Immunology, Duke University Medical Center, Durham, North Carolina, USA.

Current therapies for non-Hodgkin lymphoma commonly include CD20 mAb to deplete tumor cells. However, the response is not durable in a substantial proportion of patients. Herein, we report our studies in mice testing the hypothesis that heterogeneity in endogenous tissue CD20$^+$ B cell depletion influences in vivo lymphoma therapy. Using highly effective CD20 mAbs that efficiently deplete endogenous mature B cells and homologous CD20$^+$ primary lymphoma cells through monocyte- and antibody-dependent mechanisms, we found that lymphoma depletion and survival were reduced when endogenous host B cells were not depleted, particularly a rare IL-10–producing B cell subset (B10 cells) known to regulate inflammation and autoimmunity. Even small numbers of adoptively transferred B10 cells dramatically suppressed CD20 mAb–mediated lymphoma depletion by inhibiting mAb-mediated monocyte activation and effector function through IL-10–dependent mechanisms. However, the activation of innate effector cells using a TLR3 agonist that did not activate B10 cells overcame the negative regulatory effects of endogenous B10 cells and enhanced lymphoma depletion during CD20 immunotherapy in vivo. Thus, we conclude that endogenous B10 cells are potent negative regulators of innate immunity, with even small numbers of residual B10 cells able to inhibit lymphoma depletion by CD20 mAbs. Consequently, B10 cell removal could provide a way to optimize CD20 mAb–mediated clearance of malignant B cells in patients with non-Hodgkin lymphoma.

Introduction

Non-Hodgkin lymphoma (NHL) is a heterogeneous group of malignancies that represents approximately 4% of all cancers. More than 90% of NHLs have a B cell phenotype, and almost all express cell surface CD20 (1). A chimeric CD20 mAb, rituximab, was the first mAb to be approved for clinical use in NHL immunotherapy (2). Rituximab is given either alone or in combination with chemotherapy for the treatment of both indolent and aggressive NHL (3). Although CD20 mAb has become a standard therapy for NHL, less than 50% of patients have a durable response (4). While rituximab is effective in depleting the vast majority of circulating B cells, these only represent approximately 2% of all B cells. The levels of tissue B cell depletion are variable in both humans and primates (reviewed in ref. 5). In one study, for example, more than 10% of oncology patients given rituximab at high concentrations did not respond, with circulating B cells remaining in some patients (6). Even among patients exhibiting some blood B cell depletion, there can be considerable heterogeneity. Similar results have been obtained in lupus patients, highlighting the potential variability of B cell depletion by rituximab in the treatment of autoimmune disease (7). Other than for Fc receptor polymorphisms in some patients (8, 9), molecular explanations for variable responses remain unknown (4), but are undoubtedly due to inconsistency in the strength of effector mechanisms among patients and molecular variability among tumors. The lack of mechanisms that explain patient variability has been a barrier to advances in the field. The current study therefore examined the relative influence of remnant endogenous B cells as positive or negative regulators of lymphoma depletion following CD20 immunotherapy.

In addition to antibody production, B cells can have both positive and negative regulatory activities (10). B cells can function as costimulatory antigen-presenting cells to induce CD4$^+$ T cell activation and differentiation, which can contribute to autoimmune disease (11). In contrast, specific B cell subsets can also negatively regulate immune responses in mice, validating the existence of regulatory B cells (12–16). A subset of regulatory B cells, termed *B10 cells*, was recently found to limit T cell–dependent inflammation and autoimmune disease through the production of IL-10 (17, 18), a potent regulatory cytokine (19). Although regulatory B10 cells only represent 1%–4% of spleen B cells, they negatively regulate the severity of autoimmune disease and inflammation (17, 18). Human B10 cells and regulatory B cells that parallel their mouse counterparts have also been described (20, 21). Given the positive and negative regulatory properties of endogenous B cells and B10 cells, their incomplete in vivo depletion during CD20 mAb treatment may directly influence lymphoma immunotherapy and contribute to patient variability.

Whether endogenous B cells can influence in vivo lymphoma therapy was examined using WT and CD20-deficient (*Cd20*$^{-/-}$) mice, since mechanistic studies are not possible in humans. B cell and immune system development are normal in *Cd20*$^{-/-}$ mice (22). Highly effective CD20 mAbs can efficiently deplete endogenous mature B cells and homologous CD20$^+$ primary lymphoma cells in WT mice with otherwise normal immunity through monocyte- and antibody-dependent mechanisms (23, 24). In this study, however, endogenous B cells in *Cd20*$^{-/-}$ mice or IL-10 production by small

Authorship note: Mayuka Horikawa and Veronique Minard-Colin contributed equally to this work and share first authorship.

Conflict of interest: Thomas F. Tedder is a paid consultant for MedImmune Inc. and a consultant for and shareholder in Angelica Therapeutics Inc.

Citation for this article: *J Clin Invest.* 2011;121(11):4268–4280. doi:10.1172/JCI59266.

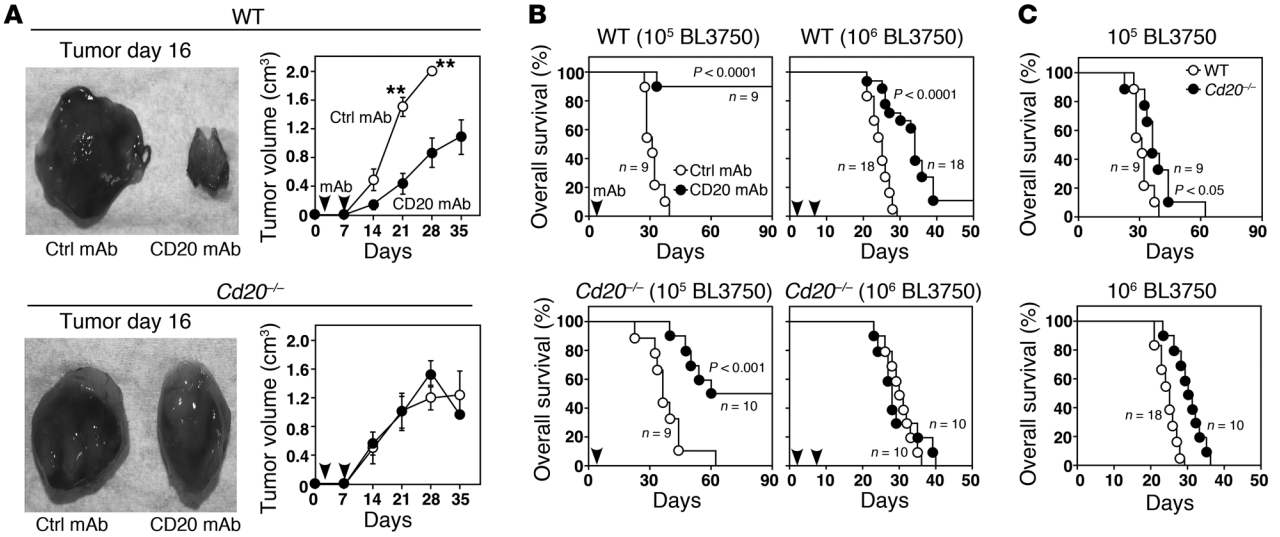

Figure 1

Endogenous B cells inhibit lymphoma depletion by CD20 mAbs in vivo. (**A**) Representative dorsal tumors resected from control (Ctrl) or CD20 mAb–treated WT or *Cd20*$^{-/-}$ mice 16 days after receiving 10^6 BL3750 cells. Line graphs indicate tumor volumes for mice given CD20 (black circles) or control (white circles) mAbs (250 μg/mouse) on days 1 and 7 (arrowheads) following the transfer of 10^6 BL3750 cells. Values represent mean tumor volumes observed in 3–6 mice for each group from 2 independent experiments. (**B**) Survival of WT or *Cd20*$^{-/-}$ mice given 10^5 (left panels) or 10^6 (right panels) BL3750 cells on day 0, with CD20 (black circles) or control (white circles) mAbs given on day 1 or days 1 and 7 (arrowheads) in 3 or more independent experiments. Significant cumulative survival differences between groups treated with CD20 versus control mAbs are indicated. All mice that survived more than 90 or 50 days (as shown) remained disease free for 6 or more months. (**C**) Survival of WT and *Cd20*$^{-/-}$ mice given 10^5 or 10^6 BL3750 cells on day 0. Significant cumulative survival differences between WT and *Cd20*$^{-/-}$ mice are indicated. Data represent mean ± SEM.

numbers of adoptively transferred B10 cells inhibited lymphoma clearance and reduced survival in mice given CD20 mAbs. Mouse B10 cell inhibition of lymphoma clearance by CD20 mAbs was explained by their ability to negatively regulate monocyte activation, a property shared with human B10 cells (20). Therefore, B10 cells are potent negative regulators of innate immune responses and their removal is essential for optimal CD20 mAb clearance of malignant B cells in vivo.

Results

Endogenous B cells inhibit lymphoma immunotherapy. The role of endogenous B cells during lymphoma immunotherapy was examined using mouse anti-mouse CD20 mAbs (MB20-11) and mouse CD20-expressing primary Burkitt-like lymphoma cells isolated from a syngeneic *Eμ-cMycTG*$^{+/-}$ mouse (23). A single dose of MB20-11, but not control mAbs (250 μg/mouse), depletes more than 95% of mature B cells in lymphoid tissues of WT mice after 7 days, with the effect lasting up to 8 weeks (5, 23–29). WT mice given 10^5 BL3750 cells on day 0 developed detectable tumors at the site of injection by 12–19 days, with a 31-day median survival (range 27–39; Figure 1, A and B). CD20 mAbs given to WT mice 1 day after BL3750 cell transfers had a significant therapeutic effect on tumor growth, with 89% of mice remaining disease free for 60 days or longer ($P < 0.0001$). Transplantation of 10^6 BL3750 cells resulted in death of all control mAb-treated mice (median 25 days, range 21–29). CD20 mAb treatment on days 1 and 7 delayed tumor growth and extended median survival by 36% (34 days, $P < 0.0001$). In contrast, CD20 mAb treatment of *Cd20*$^{-/-}$ mice did not deplete endogenous B cells and only induced survival in 50% of mice given 10^5 CD20$^+$ BL3750 cells ($P < 0.001$). Tumor growth and survival were equivalent in *Cd20*$^{-/-}$ mice given 10^6 BL3750 cells regardless of CD20 (median 28 days, range 23–40) or control (median 31 days, range 23–36) mAb treatment. Thus, the antitumor effects of CD20 mAbs were observed in WT mice, but not in *Cd20*$^{-/-}$ mice.

The differences in tumor immunotherapy between WT and *Cd20*$^{-/-}$ mice did not reflect variability in BL3750 tumor growth or CD20 mAb effects in vivo. There was prolonged survival of *Cd20*$^{-/-}$ mice relative to WT littermates given BL3750 cells (Figure 1C), but this is readily explained by immune responses generated against CD20 present on BL3750 cells (22). However, antitumor, anti-idiotype, or anti-CD20 mAb antibodies were not detectable in *Cd20*$^{-/-}$ mice with or without CD20 mAb treatment (data not shown). Furthermore, CD20 mAbs readily depleted more than 95% of tissue B cells in WT mice, regardless of whether they had been given BL3750 cells 1 day before mAb treatment (Figure 2A). CD20 mAbs also depleted CFSE-labeled WT B cells equally in WT and *Cd20*$^{-/-}$ recipients (Figure 2B). Thus, the persistence of endogenous B cells in *Cd20*$^{-/-}$ mice significantly inhibited the antitumor effects of CD20 mAbs that were observed in WT mice.

Small numbers of B10 cells inhibit CD20 immunotherapy. Since IL-10–competent B10 cells regulate inflammation and immune responses, their role in CD20 immunotherapy was evaluated. B10 cells are identified by their ability to express cytoplasmic IL-10 following 5 hours of in vitro stimulation with LPS, PMA, and ionomycin, with monensin included in the cultures to block IL-10 secretion (30, 31). Negative controls for IL-10 staining included isotype-matched control mAbs and B cells from IL-10–deficient (*Il10*$^{-/-}$) mice. Spleen B10 cell frequencies and numbers were equivalent in WT and *Cd20*$^{-/-}$ mice, but CD20 mAb treatment only depleted B10 cells from WT mice (>95%; Figure 3A). Remarkably, B10 cell

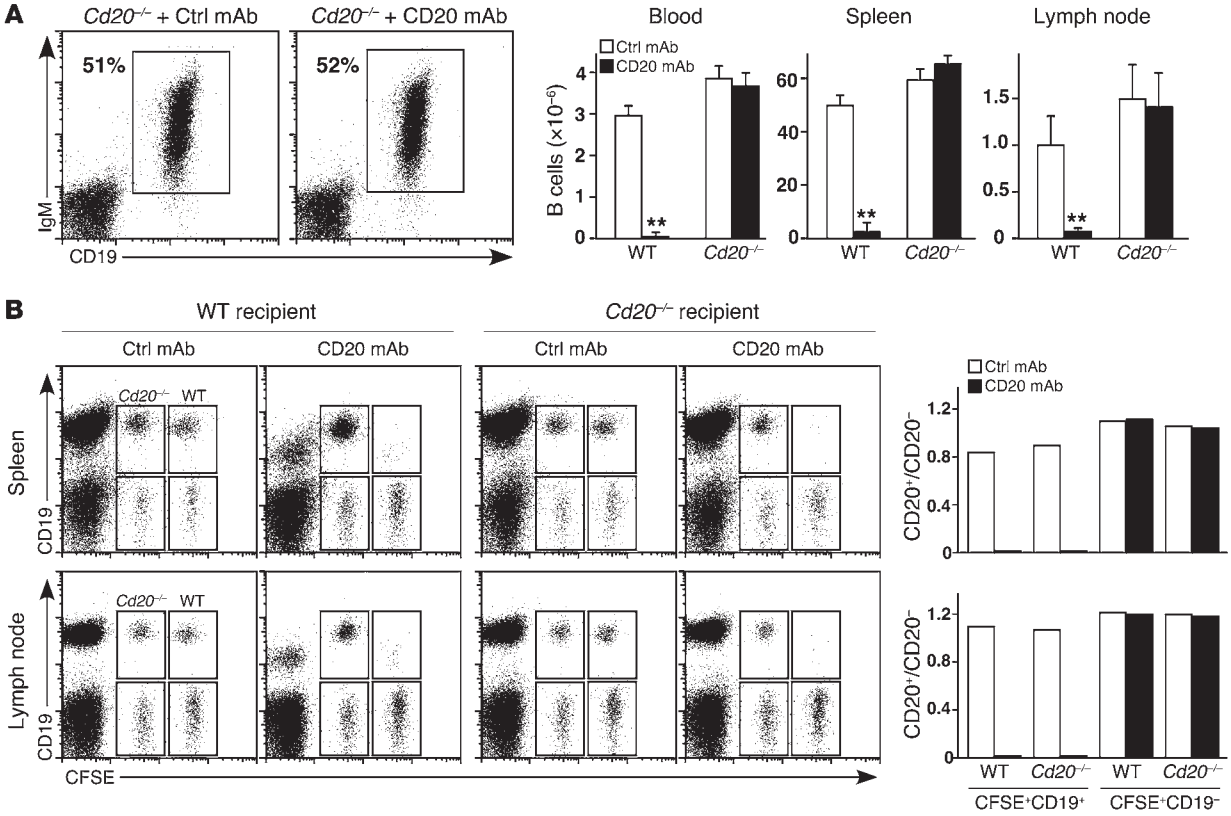

Figure 2

B cell depletion by CD20 mAbs in *Cd20*$^{-/-}$ mice. (**A**) Endogenous B cells in *Cd20*$^{-/-}$ mice are not depleted by CD20 mAbs. Values represent B220^{+} B cell numbers in WT and *Cd20*$^{-/-}$ mouse tissues 7 days after control or CD20 mAb treatment (250 μg/mouse). Identical results were also obtained in mice given 10^6 BL3750 cells 1 day before mAb treatment (data not shown). Blood numbers represent cells ×10^{-6}/ml. Values represent means for 3 mice in each group and represent 4 independent experiments. Significant differences between means are indicated. $^{**}P < 0.01$. (**B**) Efficient depletion of WT B cells by CD20 mAbs in *Cd20*$^{-/-}$ mice. *Cd20*$^{-/-}$ and WT splenocytes were CFSE labeled at different intensities, mixed equally, and transferred into WT or *Cd20*$^{-/-}$ recipients before CD20 or control mAb treatment. Spleen and peripheral lymph node lymphocytes were isolated after 3 days and stained for CD19 expression. The gates show CD19^{+} and CD19^{-} lymphocytes from WT donors (CFSE^{hi}) relative to *Cd20*$^{-/-}$ donors (CFSE^{lo}). Bar graphs indicate mean CD20^{+} to CD20^{-} cell ratios within the CFSE-labeled CD19^{+} and CD19^{-} lymphocyte populations from 2 independent experiments. Data represent mean ± SEM.

frequencies also expanded 2-fold in tumor-bearing WT (Figure 3B) and *Cd20*$^{-/-}$ mice (data not shown) by day 28. However, the relative frequency of spleen B10 cells decreased significantly as BL3750 cells displaced spleen lymphocytes, which argues that B10 cells were not required for lymphoma progression.

To determine whether B10 cells inhibited the antitumor effects of CD20 mAbs in vivo, CD1d^{hi}CD5^{+} B cells that are enriched for B10 cells and progenitor B10 (B10pro) cells or conventional non-CD1d^{hi}CD5^{+} B cells were purified from *Cd20*$^{-/-}$ mice (Figure 3C) and adoptively transferred into WT mice as described (17, 18). B10 cells represented 9%–11% of the spleen CD1d^{hi}CD5^{+} B cell subset, while B10 cells represented less than 1% of non-CD1d^{hi}CD5^{+} B cells. Therefore, the adoptive transfer of 2×10^6 CD1d^{hi}CD5^{+} B cells included approximately 2×10^5 IL-10–competent B10 cells. Recipient mice were given 10^6 BL3750 cells 1 day later (day 0), followed by CD20 or control mAb treatment. CD20 mAb treatment delayed tumor growth and prolonged survival in WT mice (median 34 days, range 21–39; $P < 0.0001$; Figure 4). However, the adoptive transfer of *Cd20*$^{-/-}$ CD1d^{hi}CD5^{+} B cells eliminated the therapeutic benefit of CD20 mAbs and reduced survival to levels observed in control mAb-treated mice (median 24 days, range 21–26). The adoptive transfer of *Cd20*$^{-/-}$ CD1d^{lo}CD5^{-} B cells was without effect.

Whether B10 cell IL-10 production was responsible for eliminating the therapeutic benefit of CD20 mAb treatment was determined using B cells from *Il10*$^{-/-}$*Cd20*$^{-/-}$ mice. The adoptive transfer of either CD1d^{hi}CD5^{+} or CD1d^{lo}CD5^{-} B cells from *Il10*$^{-/-}$*Cd20*$^{-/-}$ mice into WT mice did not affect tumor growth or mouse survival following CD20 mAb treatment (Figure 4). IL-10–competent B10 cells develop normally in *Il10*$^{-/-}$ mice, as equal numbers of CD1d^{hi}CD5^{+} B cells from WT and *Il10*$^{-/-}$ mice express an independent IL-10 reporter gene following stimulation (D. Maseda, S.H. Smith, D.J. DiLillo, J.M. Bryant, K. Candando, C.T. Weaver, T.F. Tedder, unpublished observations). Furthermore, IL-10 production by B10 cells was unlikely to influence BL3750 growth, since lymphoma progression was identical in WT and *Il10*$^{-/-}$ mice (Figure 5A and Supplemental Figure 1; supplemental material available online with this article; doi:10.1172/JCI59266DS1). Therefore, B10 cells negatively regulated CD20 mAb–induced lymphoma depletion through the production of IL-10.

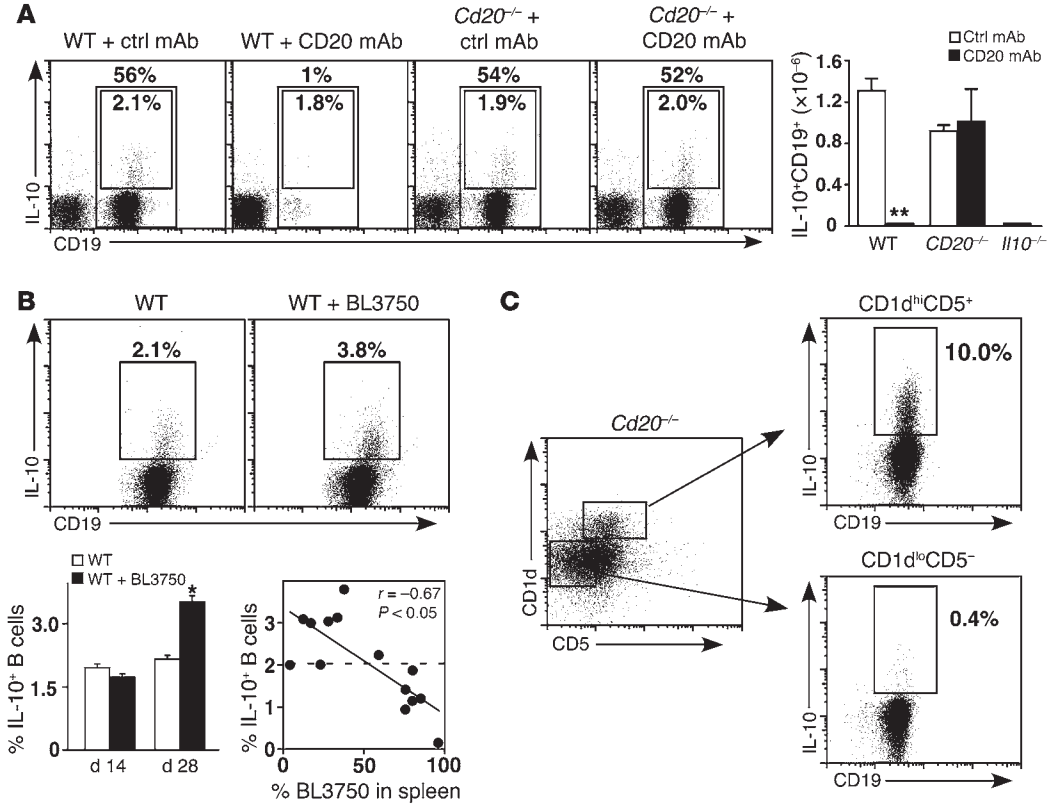

Figure 3

B10 cell subset expansion in mice with lymphoma. (**A**) Representative spleen IL-10–producing B cell frequencies in control or CD20 mAb–treated WT or *Cd20*$^{-/-}$ mice. Percentages within the gates indicate mean frequencies of IL-10$^+$ cells among CD19$^+$ B cells (bottom numbers) and the mean relative frequency of CD19$^+$ B cells among total lymphocytes (top numbers). Bar graph shows mean IL-10–producing B cell numbers 7 days after control or CD20 mAb treatment, with 3 or more mice/value from 2 experiments. Results with *Il10*$^{-/-}$ mice are shown as background controls for IL-10 staining. (**B**) Spleen B10 cell frequencies increase during lymphoma progression. Representative dot plots showing IL-10$^+$ B cell frequencies in a mouse 28 days after BL3750 cell transfer or an untreated littermate (top panels). Percentages above the indicated gates indicate IL-10$^+$ B cell frequencies. Bar graphs indicate mean percentages of B cells that produced IL-10 (n = 3 mice/group). Scatter plots compare frequencies of IL-10–producing CD19$^+$ nonmalignant B cells with lymphoma invasion (percentage of BL3750 cells among total leukocytes) from individual mice 21–35 days following BL3750 cell transfers. The dashed line indicates the mean percentage of IL-10$^+$ B cells in mice without tumors. (**A** and **B**) Significant differences between means are indicated. *P < 0.05; **P < 0.01. (**C**) Representative purification of splenic CD1d^{hi}CD5$^+$CD19$^+$ B cells from *Cd20*$^{-/-}$ mice. The frequency of IL-10–competent B10 cells within each indicated subset is shown. Percentages indicate mean IL-10$^+$ B cell frequencies as determined by flow cytometry analysis in 4 independent experiments. Data represent mean ± SEM.

B10 cells regulate macrophage activation. To determine how B10 cells regulate CD20 mAb–induced lymphoma depletion, the relative contributions of innate effector cells to lymphoma and B cell depletion by CD20 mAbs was assessed. CD20 mAbs deplete normal and malignant B cells through IgG Fc receptors (FcγR) (23, 24). Lymphoma depletion was dependent on monocytes, as their clodronate-induced depletion from tumor-bearing mice (WT/Clod) eliminated the therapeutic benefit of CD20 mAbs (Figure 5B). Likewise, macrophage depletion significantly reduced blood and spleen B cell clearance over a range of CD20 mAb concentrations (Figure 5C). Lymphoma depletion did not require endogenous B or T cells, as CD20 mAb treatment significantly prolonged the survival of *Rag1*$^{-/-}$ mice given BL3750 cells (Figure 5B). Since monocytes, neutrophils, and NK cells are required for host defense, their relative contributions to normal B cell depletion by CD20 mAbs was compared in mice without tumors. *Mcl1*$^{-/-}$ mice have 80%–86% reductions in blood and spleen neutrophils, but have normal macrophages (32). *Gfi1*$^{-/-}$ mice lack phenotypically mature neutrophils, while morphologically normal monocytes are present in normal numbers (33). Splenic B220$^+$ B cells from WT, *Mcl1*$^{-/-}$, and *Gfi1*$^{-/-}$ mice expressed cell-surface CD20 at identical levels (data not shown). NK1.1 mAb treatment reduced circulating NK cells by 93% ± 2%, as determined by DX5 mAb staining (data not shown). Nonetheless, CD20 mAb treatment depleted normal numbers of blood and spleen B cells in *Mcl1*$^{-/-}$, *Gfi1*$^{-/-}$, and NK cell–depleted mice after 7 days. Thus, CD20 mAb–induced lymphoma and B cell depletion were macrophage dependent.

Since monocytes express the IL-10 receptor at high levels (19), the effect of adoptively transferred B10 cells on monocyte activation was examined in vivo. Spleen CD1d^{hi}CD5$^+$ B cells were purified from *Cd20*$^{-/-}$ mice and transferred into WT mice that were later given BL3750 cells followed by CD20 mAbs 1 day later. Forty-eight hours after CD20 mAb treatment, activation-induced upregulation of major histocompatibility class II molecules and CD86 expression were significantly reduced on splenic CD11b$^+$ cells from mice given *Cd20*$^{-/-}$ CD1d^{hi}CD5$^+$ B cells (Figure 6A). LPS-induced nitric

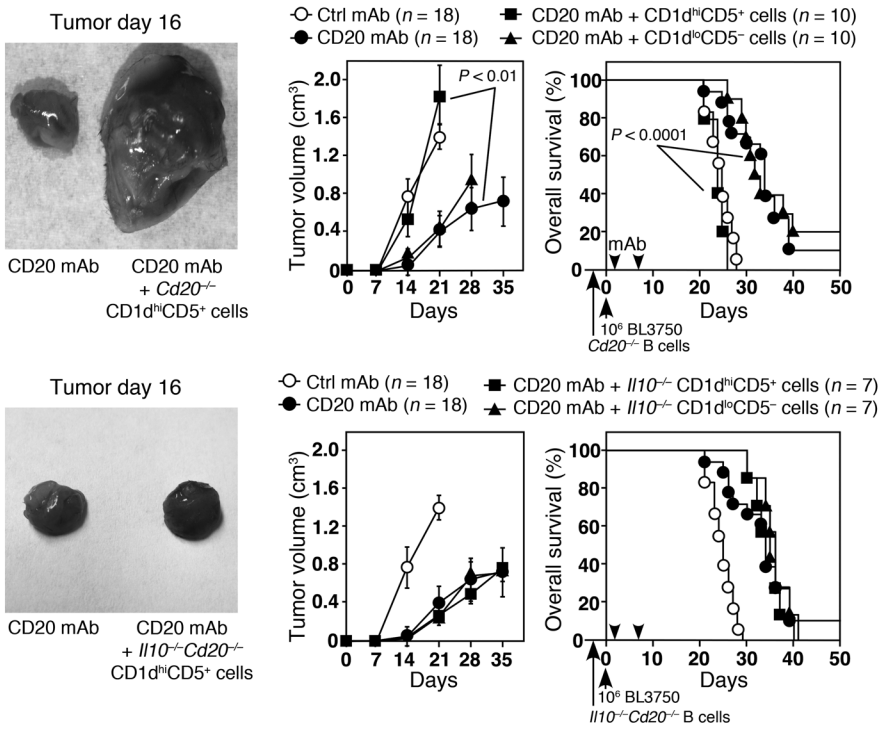

Figure 4

B cell IL-10 production inhibits lymphoma depletion by CD20 mAbs in vivo. CD1d^{hi}CD5^{+} B cells inhibit lymphoma depletion by CD20 mAbs through IL-10 production. B cell subsets purified from *Cd20*$^{-/-}$ or *Il10*$^{-/-}$*Cd20*$^{-/-}$ mice were transferred into WT recipients (2×10^6/mouse) 1 day before the mice were given 10^6 BL3750 tumor cells on day 0. CD20 or control mAbs (250 μg) were given on days 1 and 7 (arrowheads). Representative dorsal tumors were resected from mice on day 16. Tumor volumes and cumulative mouse survival were quantified after tumor challenge and control (white circles), CD20 mAb (black circles), CD20 mAb plus CD1d^{hi}CD5^{+} B cell (squares), or CD20 mAb plus non-CD1d^{hi}CD5^{+} B cell (triangles) treatments. Results represent pooled data from 4 independent experiments. Significant cumulative survival differences between groups given CD1d^{hi}CD5^{+} or non-CD1d^{hi}CD5^{+} B cells are shown. All mice that survived more than 50 days remained disease free for 6 or more months. Data represent mean ± SEM.

oxide and TNF-α production were also significantly reduced when bone marrow CD11b^{+} cells or peritoneal macrophages were cocultured with CD1d^{hi}CD5^{+} B cells, but were significantly increased when the cells were cocultured with CD1d^{lo}CD5^{-} B cells (Figure 6, B–D). CD1d^{hi}CD5^{+} B cell regulation of nitric oxide and TNF-α production was completely IL-10 dependent (Figure 6, B and D). Thus, CD1d^{hi}CD5^{+} B cells can significantly reduce monocyte activation in vivo and in vitro.

TLR activation enhances CD20 mAb efficacy in vivo. Since monocyte activation may bypass B10 cell–negative regulation in WT mice, the ability of TLR stimulation to enhance lymphoma depletion was evaluated. TLR3 (polyinosinic-polycytidylic acid; poly[I:C]), TLR4 (LPS), and TLR9 (CpG) agonists induced significant TNF-α production by bone marrow CD11b^{+} cells (Figure 7A) and induced higher FcγRII/III expression levels on spleen macrophages, neutrophils, and NK cells (Figure 7B).

Whether TLR agonists could also augment B cell depletion in vivo was determined in mice given limited amounts of MB20-11 CD20 mAbs, with peritoneal cavity B cells enumerated 7 days later. Peritoneal cavity B cells are normally refractory to CD20 mAb–induced depletion due to the low number of endogenous monocytes (5). However, giving mice TLR agonists significantly enhanced the removal of peritoneal B cells in a CD20 mAb dose-dependent manner (Figure 7, C and D). These TLR agonists also significantly induced B cell depletion in response to a CD20 mAb (MB20-1, IgG1) that is less efficient at FcγR engagement than MB20-11 mAbs (24). CD20 mAb treatment alone reduced peritoneal B2 cell numbers significantly, while peritoneal B1a and B1b B cells were less affected (Figure 7D). However, 98%, 82%–93%, and 94%–95% of peritoneal B2, B1a, and B1b cells, respectively, were depleted by CD20 mAbs in mice given TLR agonists. The ability of CpG to enhance peritoneal B cell depletion by CD20 mAbs was significantly reduced by MyD88 deficiency (Figure 7E), which reduces TLR4 and TLR9 signaling (34). Thus, TLR signaling significantly enhanced CD20 mAb–induced B cell depletion under conditions in which B cell clearance was limited.

Poly(I:C) enhances CD20 mAb–induced lymphoma depletion. The ability of TLR activation to augment lymphoma depletion was determined in mice given BL3750 cells on day 0 followed by control mAbs plus TLR agonists on days 1, 7, 14, and 21. Only poly(I:C) significantly enhanced mouse survival (median 33 days; Figure 8A). The ability of TLR agonists to augment low-dose CD20 mAb (10 μg) effectiveness in vivo was also examined. The median survival of mice given lymphomas and CD20 mAbs alone was 33 days (range 24–43). The median survival of mice given CD20 mAbs along with LPS (42 days, $P < 0.05$) or CpG (37 days) was increased. However, the median survival of mice given CD20 mAbs along with poly(I:C) was dramatically increased (>60 days, $P < 0.001$), with this treatment preventing tumors in 62% of mice for up to 6 months. Half of mice given BL3750 cells along with low-dose CD20 mAbs and 50–500 μg of poly(I:C) weekly for 4 weeks survived, while none of the control or CD20 mAb–treated mice survived ($P < 0.01$; Figure 8B). The combination of low-dose CD20 mAbs plus poly(I:C) also significantly reduced circulating leukocyte counts ($P < 0.01$) and delayed tumor growth ($P < 0.01$) when compared with CD20 mAbs alone or control mAbs plus poly(I:C) (Figure 8, C and D). Thus, poly(I:C) uniquely enhanced the in vivo efficacy of CD20 immunotherapy.

Poly(I:C) activates monocytes but not B10 cells. Whether poly(I:C), LPS, or CpG differentially enhance CD20 mAb–induced lymphoma depletion by stimulating monocytes, BL3750 cells, B cells, or B10 cells was assessed. Poly(I:C) significantly enhanced macrophage phagocytosis of CD20 mAb–coated B cells in vitro in contrast with CD20 mAbs alone or control mAbs plus poly(I:C) (Figure 9A). LPS and CpG enhanced macrophage phagocytosis of CD20 mAb–coated B cells similarly (Supplemental Figure 2A). Poly(I:C) enhanced monocyte function by signaling through TLR3-

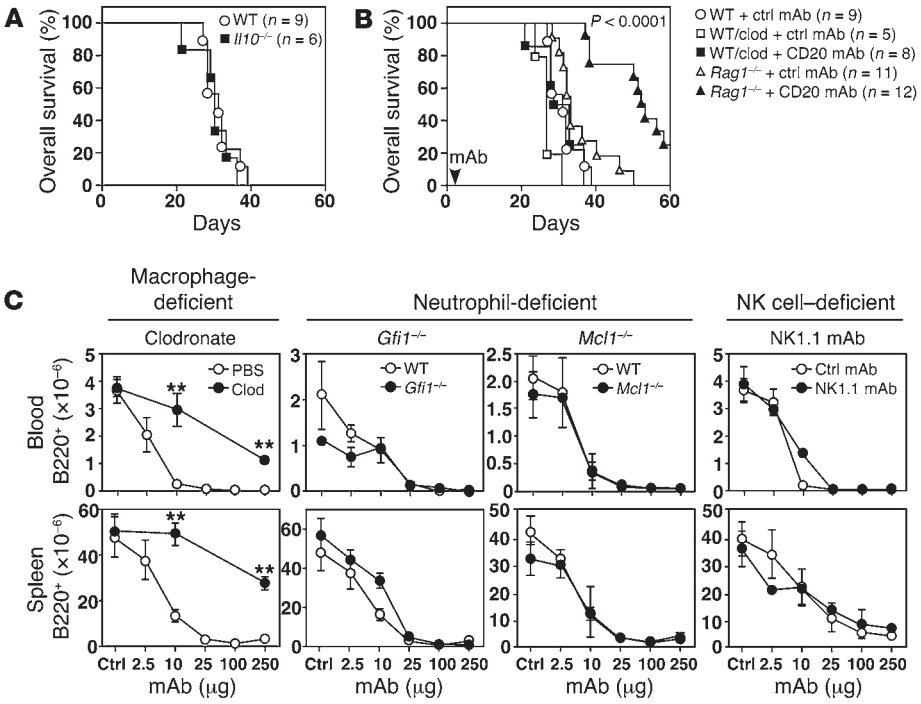

Figure 5

Macrophages mediate lymphoma depletion following CD20 mAb treatment. (**A**) IL-10 does not influence BL3750 tumor growth in vivo. WT and *Il10*$^{-/-}$ mice were given 10^5 BL3750 cells on day 0 with survival monitored thereafter. (**B**) Macrophages, but not B or T lymphocytes, mediate lymphoma depletion following CD20 mAb treatment. WT and *Rag1*$^{-/-}$ mice were given 10^5 BL3750 cells on day 0 with control or CD20 mAb (250 μg) treatment on day 1. Some mice were treated with clodronate-encapsulated liposomes to deplete macrophages before tumor transfers as indicated. Significant cumulative survival differences between control and CD20 mAb treatment groups are shown. Mice that survived more than 60 days remained disease free for 6 or more months. (**C**) Blood and spleen B cell numbers in macrophage-deficient (clodronate-treated), neutrophil-deficient (*Gfi1*$^{-/-}$ or *Mcl1*$^{-/-}$), or NK cell–deficient (anti-NK1.1 mAb–treated) mice (black circles), and their WT littermates (white circles) 7 days after CD20 (2.5–250 μg) or control (250 μg) mAb treatment. Values represent mean B cell numbers (≥3 mice per value) at the indicated mAb doses. Significant differences between means are indicated. $^{**}P < 0.01$. Data represent mean ± SEM.

and TRIF-dependent pathways, since it was unable to augment the phagocytic capacity of macrophages isolated from *Tlr3*$^{-/-}$ or *Trif*$^{-/-}$ mice (Figure 9B). Spleen B cells and BL3750 cells expressed modest if any TLR3 transcripts, while TLR4 and TLR9 transcripts were readily identified (Figure 9, C and D). Consistent with this, spleen B cells proliferated significantly in response to LPS and CpG stimulation, but not poly(I:C) ($P < 0.05$; Figure 9E). Culturing mouse spleen B cells or human blood mononuclear cells with LPS or CpG induced significant numbers of B10pro cells to mature into IL-10–secreting B10 cells, while poly(I:C) was without effect (Figure 9, F and G). These TLR agonists or IL-10 did not induce BL3750 cells to express IL-10 (Figure 9, F–H) or significantly affect BL3750 cell proliferation, survival, and CD20 expression (Supplemental Figure 2B). Thus, poly(I:C) enhanced antibody-dependent phagocytosis, while not inducing B10pro cell maturation, B10 cell IL-10 secretion, or B cell proliferation.

Poly(I:C) overcomes the inhibitory effect of endogenous B cells on CD20 immunotherapy. To determine whether poly(I:C) circumvents the negative regulatory effects of B10 cells, *Cd20*$^{-/-}$ mice were given BL3750 cells and subsequently treated with CD20 mAbs plus poly(I:C). *Cd20*$^{-/-}$ mice given either poly(I:C) or CD20 mAbs alone developed detectable tumors by 14–25 days, with a median survival of 32 and 35 days, respectively (Figure 10A). CD20 mAb plus poly(I:C) treatment significantly delayed tumor growth and extended median survival by 29% relative to CD20 mAbs alone (45 days, $P < 0.05$). Thus, poly(I:C) treatment significantly reduced the inhibitory effect of endogenous B10 cells on CD20 immunotherapy.

CD19 mAbs also deplete B cells in human CD19 transgenic mice through monocyte- and FcγR-dependent mechanisms (35, 36). Therefore, the therapeutic benefit of poly(I:C) was also tested using mouse anti-mouse CD19 mAbs and BL3750 cells, which express cell surface CD19 (23). CD19 mAbs given 1 day after transfer of BL3750 cells significantly prolonged mouse survival ($P < 0.05$; Figure 10B). Remarkably, 75% of the mice treated with poly(I:C) plus CD19 mAbs remained tumor free until the experiment was terminated at 180 days.

Whether poly(I:C) treatment could also overcome lymphoma resistance to CD20 mAb treatment was determined using a CD20 mAb–resistant CD20$^+$ subclone of BL3750 cells. High-dose CD20 mAb treatment given 1 day after the transfer of BL3750-6 cells had no therapeutic benefit in WT mice, with median survival of 33 days in control or CD20 mAb–treated mice (Figure 10C), even though BL3750 and BL3750-6 cells expressed CD20 at similar densities (Figure 10D). Nonetheless, CD20 mAb plus poly(I:C) treatment significantly prolonged survival when compared with CD20 mAb treatment alone (15% increase; Figure 10C). Thereby, poly(I:C) treatment significantly enhanced CD20 or CD19 mAb–induced lymphoma depletion in either WT or *Cd20*$^{-/-}$ mice.

Discussion

Endogenous B10 cells were found to be potent negative regulators of lymphoma depletion during CD20 immunotherapy. While the depletion of tissue B10 cells along with conventional B cells prolonged survival in WT mice given primary CD20$^+$ lymphoma cells and CD20 mAbs, the presence of even small numbers of CD1d^{hi}CD5$^+$ B10 cells, but not conventional B cells, significantly inhibited lymphoma depletion through IL-10–dependent mechanisms (Figures 1–4). The absence of tumor clearance in *Cd20*$^{-/-}$ mice was not expected, since circulating CD20 mAb levels persist longer in *Cd20*$^{-/-}$ mice than in WT littermates (5) and *Cd20*$^{-/-}$ mice can develop immune responses to CD20$^+$ tumors (25). Tissue B10 cell numbers were also increased 2-fold with lymphoma progression (Figure 3B), which mimics increased B10 cell numbers during inflammation and autoimmunity (17, 18). As a consequence, the incomplete or delayed depletion of tissue B10 cells may significantly

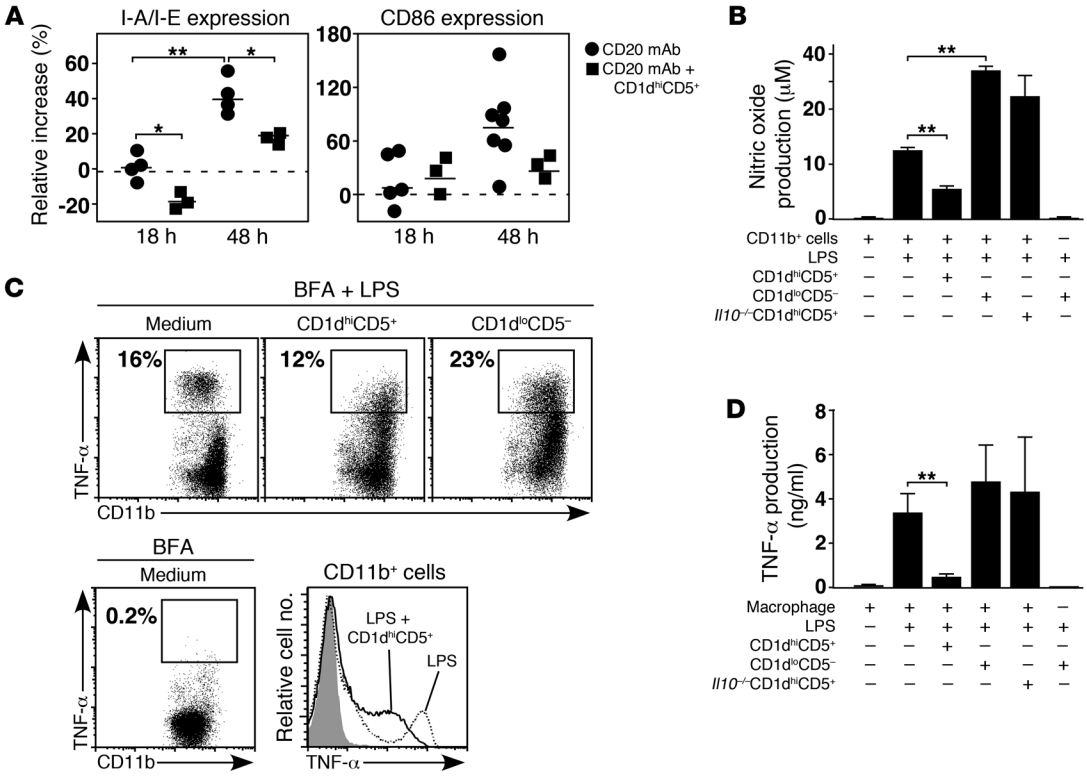

Figure 6

B10 cells regulate macrophage activation. (**A**) CD1d^{hi}CD5^{+} B cells inhibit spleen CD11b^{+} cell activation in vivo. WT mice were untreated (circles) or given 2 × 10^{6} CD1d^{hi}CD5^{+} B cells from *Cd20*$^{-/-}$ mice (squares) 1 day before BL3750 cell transfers. Mice received CD20 mAbs (250 μg) 1 day after tumor transfers. MHC class II expression by CD11b^{+}F4/80^{+}I-A/I-E^{+} cells and CD86 expression by CD11b^{+}F4/80^{+} cells were assessed 18 and 48 hours after mAb treatment. Values indicate results for individual mice (bars indicate means) relative to control mAb–treated mice (dashed lines). (**B**) CD1d^{hi}CD5^{+} B cells from WT but not *Il10*$^{-/-}$ mice inhibit nitric oxide production by CD11b^{+} cells. Splenic CD1d^{hi}CD5^{+} or CD1d^{lo}CD5^{-} B cells were cultured with LPS (10 μg/ml) overnight before culture with bone marrow CD11b^{+} cells for 48 hours, with LPS (1 μg/ml) added during the final 18 hours of culture. Values represent means from 2 independent experiments. (**C**) CD1d^{hi}CD5^{+} B cells inhibit bone marrow CD11b^{+} cell TNF-α production in vitro. Splenic CD1d^{hi}CD5^{+} or CD1d^{lo}CD5^{-} B cells were stimulated with LPS (10 μg/ml) overnight before culture with CD11b^{+} cells for 24 hours, with brefeldin A (BFA) and LPS (1 μg/ml) added during the final 4 hours of culture. Percentages indicate cell frequencies within the indicated gates. Histogram overlays show relative TNF-α expression. (**D**) CD1d^{hi}CD5^{+} B cells from WT but not *Il10*$^{-/-}$ mice inhibit peritoneal CD11b^{+} macrophage TNF-α production. The experiments were as in **C**. Values represent means from 2 independent experiments. (**A**–**D**) Significant differences between means are shown. *P < 0.05; **P < 0.01. Data represent mean ± SEM.

reduce the effectiveness of CD20 immunotherapy in some lymphoma patients, as also occurs with Fc receptor polymorphisms. In support of this, endogenous B cell depletion by CD20 mAbs is significantly reduced in NOD mice that also have elevated B10 cell numbers (29, 30). While our most potent anti-mouse CD20 mAb depletes most mature B cells efficiently in C57BL/6 mouse tissues, this may not be the case for current human CD20 therapies (6, 7). Thus, the effective removal or functional inactivation of tissue B10 cells may significantly augment lymphoma depletion during human CD20 immunotherapy.

That mouse and human B10 cell IL-10 production regulate macrophage activation in vivo and in vitro (Figure 6 and ref. 20) provides a mechanistic explanation for B10 cell regulatory effects during lymphoma immunotherapy. Macrophages serve as the primary in vivo mediators of CD20 mAb–dependent lymphoma depletion in mice (Figure 5 and ref. 23). Monocytes are also critical for rituximab clearance of human lymphoma xenografts in nude mice (37). Therefore, inducing macrophage activation but not B10 cell IL-10 production through the provision of poly(I:C) along with CD20 mAbs significantly enhanced lymphoma depletion (Figures 8 and 10). Poly(I:C) activates human and mouse monocytes/macrophages through its intracellular TLR3 receptor– and TRIF-dependent signaling pathways (38), while B cell TLR3 expression and its functional effects on B cells were modest (Figure 9, C–G, and refs. 39, 40). Poly(I:C), LPS, and CpG enhanced innate immune cell FcγR expression and induced their production of TNF-α (Figure 7, A and B) and IFN-γ (data not shown) in vitro, but cell-surface TLR4 and TLR9 are broadly expressed by most leukocytes (41). However, TLR4 and TLR9 agonists also induced B10 cell expansion and IL-10 production, which may explain in part why LPS and CpG only modestly enhanced CD20 mAb–induced lymphoma depletion. The varied effects of these 3 TLR agonists on antitumor therapy may also have involved their differential effects on regulatory or effector T cells as well as the effects of B10 cells on immune cells other than macrophages, but did not appear to result from direct effects on BL3750 tumor cells (Figure 9, F–H, and Supplemental Figure 2). Thus, selective monocyte but not B10 cell activation may provide new pathways

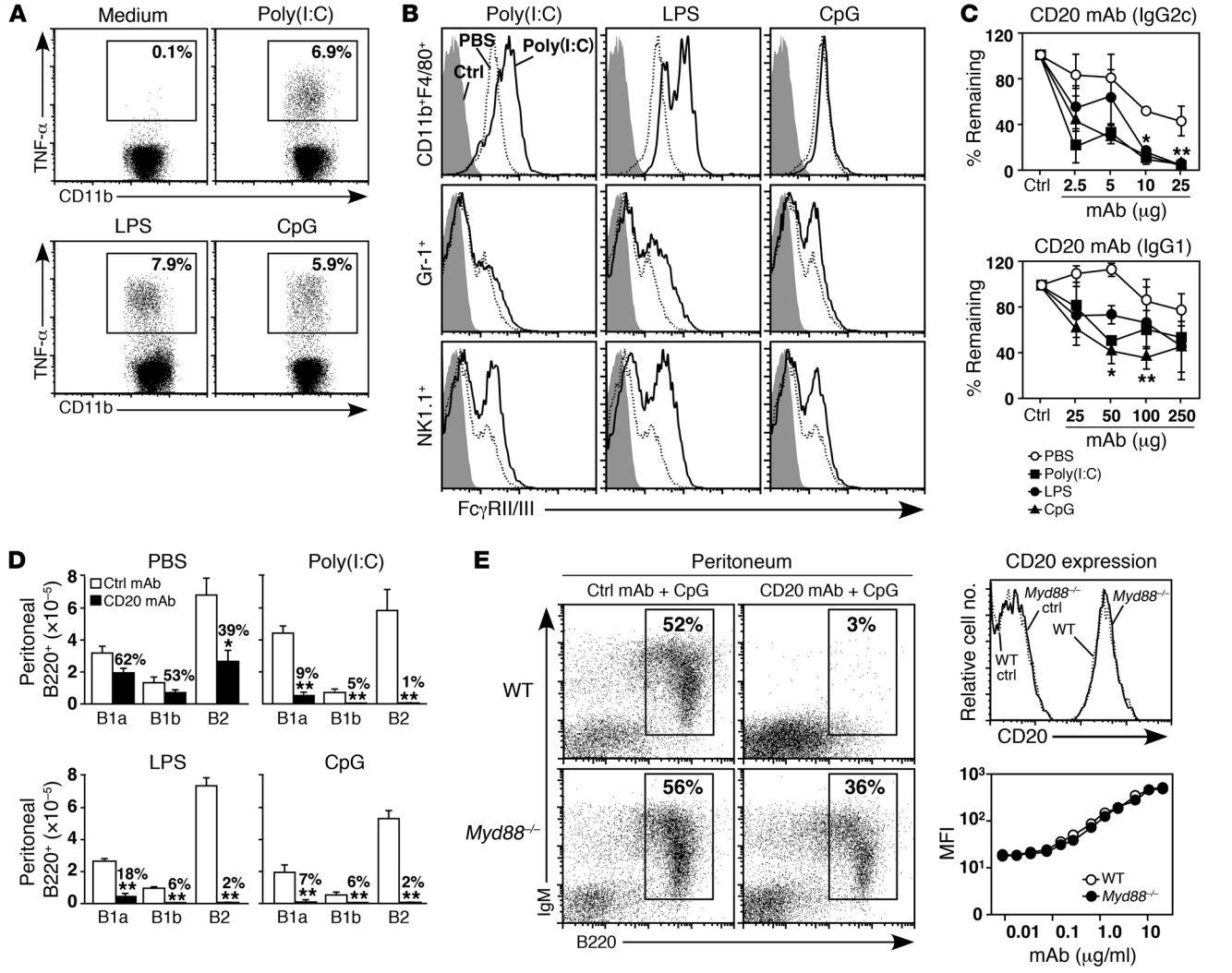

Figure 7

TLR agonists enhance CD20 mAb–induced B cell depletion. (**A**) Representative TLR-induced TNF-α production by bone marrow CD11b$^+$ cells cultured with brefeldin A for 4 hours. (**B**) Representative FcγR expression by spleen CD11b$^+$F4/80$^+$ macrophages, Gr-1$^+$ neutrophils, and NK1.1$^+$ NK cells following PBS or TLR agonist treatment. FcγRII/III expression was analyzed by ex vivo immunofluorescence staining 18 hours after the mice were treated. (**A** and **B**) Results represent 2 independent experiments. (**C**) TLR agonists enhance peritoneal cavity B cell depletion by CD20 mAbs. Mice were given CD20 (MB20-11, IgG2c; or MB20-1, IgG1) or isotype control mAbs plus PBS (white circles), poly(I:C) (squares), LPS (black circles), or CpG (triangles). Values represent mean B220$^+$ cell numbers in CD20 versus control mAb-treated mice after 7 days (≥3 mice/value). (**D**) Peritoneal B1a (CD5$^+$ CD11b$^+$IgM^{hi}B220^{lo}), B1b (CD5$^-$CD11b$^+$IgM^{hi}220^{lo}), and B2 (CD5$^-$CD11b$^-$IgM^{hi}B220^{hi}) cell numbers in mice 7 days after CD20 (MB20-11, black bars) or control (white bars) mAb (25 μg) treatment plus PBS, poly(I:C), LPS, or CpG (≥3 mice per value). (**E**) CpG does not augment peritoneal cavity B cell depletion by CD20 mAbs (MB20-11, 25 μg) in *Myd88*$^{-/-}$ mice. Percentages represent mean B220$^+$ cell frequencies 7 days after CD20 mAb treatment relative to control mAb-treated littermates (≥3 mice per value). CD19$^+$ B cells from WT and *Myd88*$^{-/-}$ mice express similar cell-surface CD20 densities as assessed over a range of CD20 mAb concentrations relative to control mAbs (10 μg/ml) binding. (**C**–**E**) Significant differences between sample means are indicated. *$P < 0.05$; **$P < 0.01$. Results represent 3–4 independent experiments. Data represent mean ± SEM.

for augmenting innate immune effector functions during CD19 and CD20 mAb and other FcγR-dependent therapies.

The current studies provide new understanding of the factors and molecular mechanisms regulating the efficacy of CD20 immunotherapy in vivo, with new findings that may be translatable into therapeutic use. Augmenting CD20 mAb effects through TLR3 agonists may be particularly advantageous when B10 cell or tumor cell numbers are significant, when tumors express CD20 at low densities, when host FcγR expression or function is compromised, or when monocyte numbers or function is reduced. Although poly(I:C) is not used clinically because of its demonstrated toxicities in mice and humans (42, 43), poly(I:C)-like agents are available for therapeutic use. As examples, poly-ICLC (Hiltonol), poly I:poly $C_{12}U$ (Ampligen, Oragen, atvogen), and poly I–mercapto poly C (polyI:MPC) have well-characterized side effects and safety profiles (44–49). Rituximab-induced cellular cytotoxicity against tumor targets is improved significantly by the addition of poly I:poly $C_{12}U$ to in vitro blood cell cultures (50). Combining poly(I:C)-

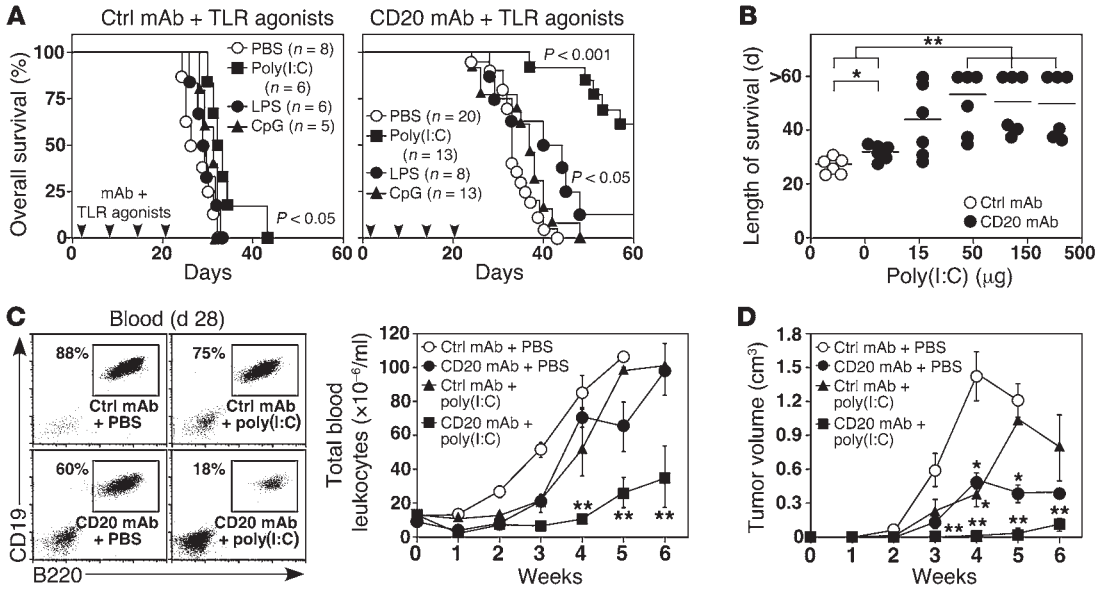

Figure 8

Poly(I:C), but not LPS or CpG, enhances lymphoma depletion by CD20 mAbs. (**A**) Poly(I:C) enhances CD20 mAb–induced lymphoma depletion. Control or CD20 mAbs (10 μg) were given concurrently with PBS (white circles), poly(I:C) (squares), LPS (black circles), or CpG (triangles) on days 1, 7, 14, and 21 following 10^5 BL3750 cell transfers. Significant cumulative survival differences between groups are indicated. B cell depletion kinetics for 10 μg MB20-11 mAbs have been described (24, 29). (**B**) Individual and mean (horizontal bars) mouse survival following BL3750 cell transfers with control (white circles) or CD20 mAbs (black circles) plus poly(I:C) treatment over a range of concentrations (0–500 μg, 6 mice/group). (**C**) Poly(I:C) enhances circulating tumor cell depletion by CD20 mAbs. Representative $CD19^+B220^+$ cell clearance 28 days following BL3750 cell transfers for the mice shown in **A**, with the relative frequencies of cells within the gates indicated. Line graphs indicate mean blood leukocyte numbers. (**D**) Tumor volumes for the mice shown in **A**. (**A** and **B**) All mice that survived more than 60 days remained disease free for 6 or more months. (**B**–**D**) Significant differences between sample means or mice treated with CD20 mAbs alone compared with CD20 mAbs plus poly(I:C) are indicated. $^*P < 0.05$, $^{**}P < 0.01$. (**C** and **D**) At time points where insufficient numbers of mice treated with control mAb had not survived for statistical analysis, comparisons were made between mice treated with CD20 mAb plus poly(I:C) versus pooled results for viable mice treated with either CD20 mAb or poly(I:C) alone. Data represent mean ± SEM.

related drugs with CD20 mAbs may also provide new therapeutic approaches for chronic lymphocytic leukemia and other B cell malignancies that are intrinsically resistant to CD20 mAb therapy (51, 52). Therefore, B10 cell depletion or B10 cell– or TLR3-directed drugs may represent powerful therapeutic approaches for enhancing CD19, CD20, and other mAb treatments for lymphoma and potentially other cancers.

LPS and CpG treatments modestly improved the outcome of CD20 immunotherapy (Figure 8A). However, CpG treatment does enhance the efficacy of an anti-IgM idiotype mAb against murine B cell lymphoma by enhancing NK cell and granulocyte antibody-dependent killing in vitro (53, 54). Furthermore, CpG treatment is reported to increase CD20 expression by malignant B cells (55). Based on these findings, a phase I clinical trial for CpG in combination with rituximab treatment weekly for 4–20 weeks was carried out in patients with relapsed/refractory $CD20^+$ B cell NHL (56, 57). Combined CpG and rituximab treatments were well tolerated and without major toxicities. Nevertheless, the use of TLR9 agonists may be complicated, since B cell–derived lymphomas and normal B cells express TLR9 (Figure 9, C and D, and ref. 58). Furthermore, repeated CpG administration has negative consequences in mice, including severely altered morphology and functionality of lymphoid organs, multifocal liver necrosis, and hemorrhagic ascites (59). In contrast, repetitive poly(I:C) challenge is not immunotoxic or hepatotoxic in mice (59). Blocking B10 cell function by providing an IL-10–neutralizing antibody systemically (17) is unlikely to prove effective long-term, since IL-10 is an important regulatory cytokine that is produced by a large number of hematopoietic and nonhematopoietic cells as part of multiple diverse regulatory circuits (19). Moreover, IL-10–deficient mice develop multiple manifestations of heightened cellular and humoral immunity, which eventually lead to systemic inflammation and autoimmunity. Thus, poly(I:C)-like TLR agonists may be preferred agents for enhancing CD20 mAb efficacy in vivo.

These studies demonstrate that optimal lymphoma depletion during immunotherapy involves at least 2 mechanisms: direct CD20 mAb targeting of tumor cells for depletion by monocytes and enhanced tumor depletion by the removal of endogenous B10 cells. B10 cells may also negatively regulate other tumor-specific immune responses. For example, CD20 mAb removal of endogenous B10 cell–negative regulation may explain the recent observation that B cell depletion prior to adoptive immunotherapy with T cells expressing CD20-specific chimeric T cell receptors facilitates the eradication of leukemia in immunocompetent mice (60). Preferential B10 cell depletion in mice also significantly enhances both cellular and humoral immune responses (61, 62). Enhanced immunity and resistance to diverse syngeneic tumors has also been reported in congenitally B cell–deficient μMT mice (63–65). The significant role for B10 cells in mAb-mediated tumor depletion provides an additional explanation for these previous studies and identifies an

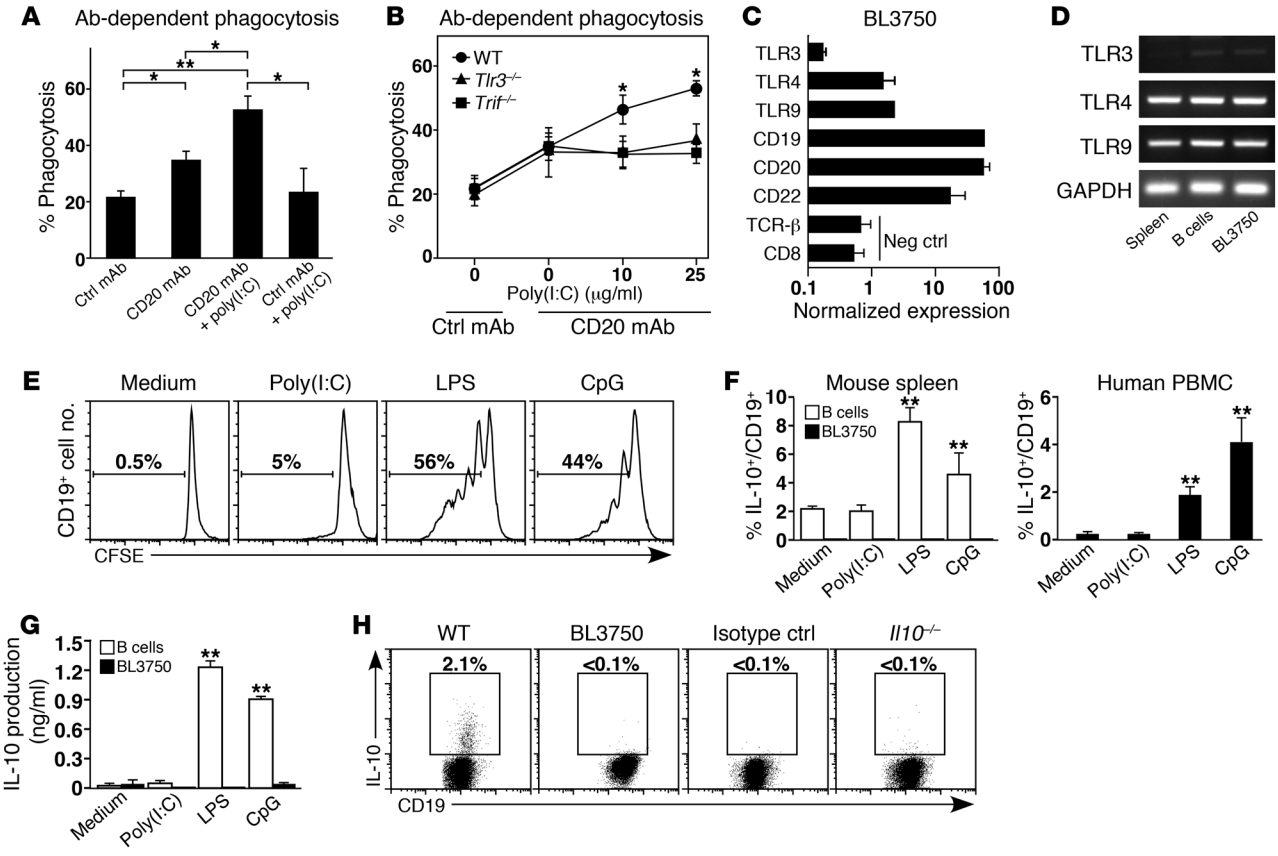

Figure 9

Poly(I:C) does not induce B10 cell proliferation or IL-10 production. (**A**) Poly(I:C) enhances antibody-dependent monocyte phagocytosis of spleen B cells in vitro that is (**B**) TLR3 and TRIF dependent. Phagocytosis of CD20 mAb–coated CFSE-labeled B cells by poly(I:C)-treated macrophages was assessed by flow cytometry. Values indicate mean frequencies of monocytes containing CFSE-labeled B cells from 3–5 independent experiments. (**C**) TLR gene expression by BL3750 cells. Relative mean transcript levels are indicated. (**D**) TLR transcript expression by BL3750 cells, whole spleen, and purified spleen B cells was assessed by PCR amplification. GAPDH was used as a positive control. (**E**) Poly(I:C) does not induce spleen B cell proliferation. CSFE-labeled B cells were cultured with TLR agonists for 72 hours. Representative frequencies of dividing CD19+ cells are shown. (**F**) BL3750, mouse spleen (n = 3–5/group), or human blood mononuclear (n = 10–12/group) cells were stimulated for 48 hours with LPS, CpG, or poly(I:C), with PMA, ionomycin, and brefeldin A added for the last 5 hours of culture. Bar graphs indicate IL10+ B cell frequencies. (**G**) Poly(I:C) does not induce BL3750 or B cell IL-10 secretion. BL3750 or spleen B cells were cultured with medium alone or TLR agonists for 72 hours, with IL-10 concentrations quantified by ELISA. (**H**) BL3750 cells do not express cytoplasmic IL-10 after 5 hours of in vitro stimulation, relative to WT and *Il10*$^{-/-}$ mouse splenocytes. (**A**, **B**, **F**, and **G**) Significant differences between means are indicated. *P < 0.05; **P < 0.01. (**B**–**F**) Results represent 2 or more independent experiments. Data represent mean ± SEM.

unanticipated mechanism through which human CD20-directed therapies can be optimized for lymphoma treatment.

Methods

Mice. *Cd20*$^{-/-}$ mice were as described (22). C57BL/6 mice were from NCI-Frederick Laboratory. *Il10*$^{-/-}$ (B6.129P2-*Il10*^{tm1Cgn}/J) and *Rag1*$^{-/-}$ (B6.129S7-*Rag1*^{tm1Mom}/J) mice were from the Jackson Laboratory. *Mcl1*$^{-/-}$ mice were as described (32). *Gfi1*$^{-/-}$ mice (33) were provided by H. Hock (Center for Cancer Research, Massachusetts General Hospital, Boston, Massachusetts, USA). TLR3$^{-/-}$ (B6;129S1-*Tlr3*^{tm1Flv}/J) and TRIF$^{-/-}$ (C57BL/6J-*Ticam1*^{Lps2}/J) mice were from the Jackson Laboratory. *Myd88*$^{-/-}$ mice (66) were provided by S. Akira (Osaka University, Osaka, Japan). Mice were housed in a specific pathogen–free barrier facility and first used at 6–10 weeks of age.

Immunofluorescence analysis. CD20 and CD22 expression were visualized using biotin-conjugated CD20 (MB20-11) (22) or CD22 (MB22-8) (67) plus PE-Cy5 streptavidin (eBioscience). Other mAbs included the following: B220 (RA3-6B2), CD1d (1B1), CD5 (53-7.3), CD19 (1D3), NK1.1 (PK136), and I-A/I-E (M5/114.15.2) from BD Biosciences. CD11b (M1/70), CD86 (GL1), F4/80 (BM8), IgM (II/41), Gr-1 (RB6-8C5), and IL-10 (JES5-16E3) mAbs were from eBioscience. TNF-α (MP6-XT22) mAb was from Biolegend. For immunofluorescence analysis, single-cell suspensions (10^6 cells) were stained at 4°C using predetermined optimal concentrations of mAb for 30 minutes as described (68).

For IL-10 detection, mouse spleen or blood mononuclear cells, BL3750 tumor cells, or human blood was resuspended (2×10^6 cells/ml) in complete medium (RPMI 1640 medium [Cellgro] containing 10% FCS [Sigma-Aldrich], 200 μg/ml penicillin, 200 U/ml streptomycin, 4 mM L-glutamine [all Cellgro], and 55 μM 2-mercaptoethanol [Invitrogen]) (with LPS [10 μg/ml, *E. coli* serotype 0111: B4, Sigma-Aldrich]), phorbol myristate acetate (PMA, 50 ng/ml; Sigma-Aldrich), ionomycin (500 ng/ml; Sigma-Aldrich), and monensin (2 μM; eBioscience) for 5 hours as described (31). B10 progenitor cells were induced to mature and acquire IL-10 competence in vitro by culturing the cells with LPS (10 μg/ml), CpG (human ODN 2006, 10 μg/ml, InvivoGen; mouse ODN 1668, 10 μg/ml, Integrated DNA Tech-

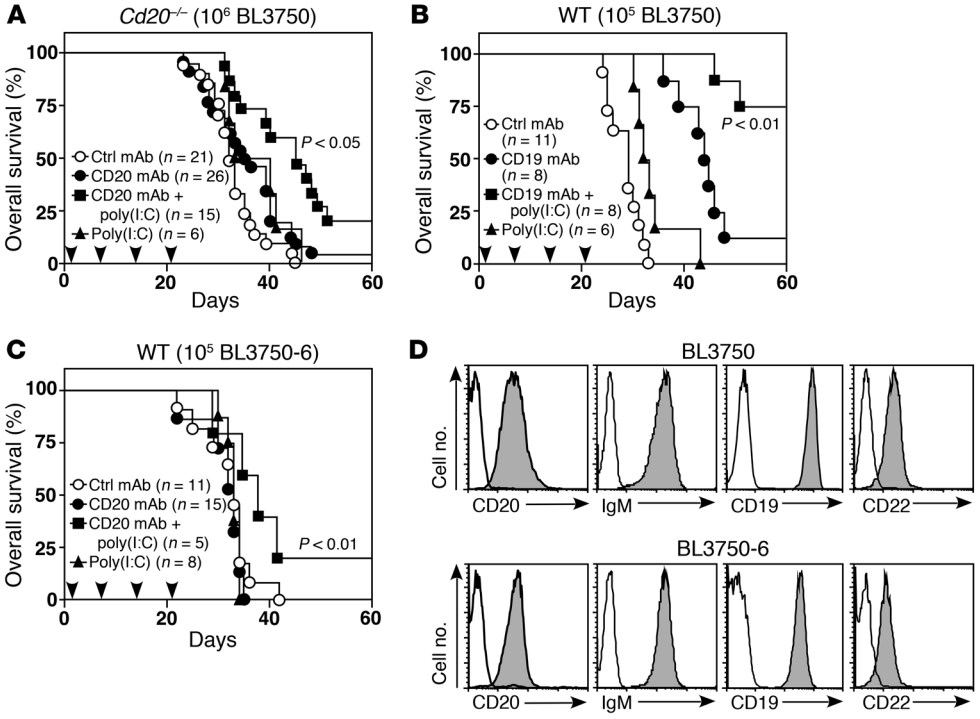

Figure 10

TLR3 activation enhances CD20 and CD19 mAb immunotherapy for lymphoma. (**A**) Poly(I:C) significantly enhances CD20 mAb efficacy and survival in *Cd20*$^{-/-}$ mice following BL3750 cell (10^6 cells/mouse) transfers. (**B**) Poly(I:C) significantly enhances CD19 immunotherapy in WT mice given 10^5 BL3750 cells. (**C**) Poly(I:C) significantly enhances survival in WT mice given 10^5 CD20 mAb–resistant BL3750-6 lymphoma cells. (**A**–**C**) Mice were given BL3750 cells 1 day before isotype control mAb (white circles, 250 μg), CD20 (250 μg), or CD19 (100 μg) mAb (black circles) treatments. Poly(I:C) (squares, triangles, 150 μg) was either given alone or with mAbs on days 1, 7, 14, and 21 (arrowheads). Significant cumulative survival differences between groups treated with mAbs plus poly(I:C) versus CD20/CD19 mAb alone and poly(I:C) alone are indicated. All mice that survived more than 60 days remained disease free for 6 or more months. (**D**) BL3750 and BL3750-6 cell-surface CD20, IgM, CD19, and CD22 expression (shaded histogram). Control mAb background staining is shown (thin line), with similar results from 3 or more experiments. Data represent mean ± SEM.

nologies), or poly(I:C) (Invivogen) for 48 hours at 37°C in a tissue culture incubator with 5% CO_2 atmosphere, with the addition of monensin, PMA, and ionomycin for the last 5 hours of culture. For TNF-α detection, bone marrow cells were resuspended (2×10^6 cells/ml) in complete medium with brefeldin A (1 μl; Biolegend) and TLR agonists (25 μg/ml) for 4 hours. Before cell-surface staining, Fc receptors were blocked using Fc receptor mAbs (2.4G2; BD Biosciences), and dead cells were labeled using a LIVE/DEAD Fixable Violet Dead Cell Stain Kit (Invitrogen–Molecular Probes). Stained cells were fixed and permeabilized using a Cytofix/Cytoperm kit (BD Biosciences) according to the manufacturer's instructions and stained with anti–IL-10 or anti–TNF-α mAbs. Isotype-matched mAbs or splenocytes from *Il10*$^{-/-}$ mice served as negative controls for IL-10 staining to demonstrate specificity and to establish background IL-10 staining levels. Isotype-matched mAbs or cells cultured with brefeldin A only served as negative controls for TNF-α staining. Human blood was obtained with informed consent according to protocols approved by the Institutional Review Board of Duke University.

CD20 immunotherapy and TLR agonist treatments. Sterile mouse anti-mouse CD20 mAbs MB20-11 (IgG2c) and MB20-1 (IgG1), and unreactive mouse control IgG2a and IgG1 mAbs were as described (24). In some experiments, mice were treated with anti-NK1.1 mAbs (100 μg) on day –4 and day 3 for NK cell depletion. Antibodies were purified by protein A affinity chromatography (Amersham) and determined to be endotoxin free (Limulus Amoebocyte Lysate assay, sensitivity of 0.06 EU/ml; Cambrex Bio Science). Macrophage deficiency was generated by tail-vein injections of clodronate-encapsulated liposomes (Sigma-Aldrich) or control PBS–encapsulated liposomes (69) in 0.2 ml given on day –1 and 0.1 ml given on days 2, 5, and 9 (Figure 5B) or 0.2 ml given on days –2, 1, and 4 (Figure 5C). For TLR agonist treatment, mice were given poly(I:C) (150 μg; Sigma-Aldrich; InvivoGen), LPS (10 μg; Sigma-Aldrich), or CpG ODN 1668 (5′-tccATGACGTTCCTGAtgcT-3′ [bases in lower case are phosphorothioate], 50 μg; Integrated DNA Technologies) i.p. concurrent with PBS or mAbs. For assessing WT B cell depletion in *Cd20*$^{-/-}$ mouse studies, splenocytes from *Cd20*$^{-/-}$ and C57BL/6 mice were differentially labeled with 0.5 and 5.0 μM CFSE Vybrant CFDA SE Fluorescent Dye (Invitrogen), respectively, as described (5). C57BL/6 and *Cd20*$^{-/-}$ splenocytes were mixed in equal numbers and given to *Cd20*$^{-/-}$ or C57BL/6 mice (10^8, i.v.) 1 day before mAb (250 μg) treatment, with CFSE-labeled cell frequencies determined 3 days later.

B cell adoptive transfer experiments. Naive *Cd20*$^{-/-}$ or *Il10*$^{-/-}$*Cd20*$^{-/-}$ mice were used as B cell donors. Splenic B cells were first enriched using CD193 mAb–coated microbeads (Miltenyi Biotec) according to the manufacturer's instructions. In addition, CD1d^{hi}CD5^{+} and CD1d^{lo}CD5^{-} B cells were isolated using a FACSVantage SE flow cytometer (BD) with purities of 95%–98%. After purification, 2×10^6 cells were immediately transferred i.v. into C57BL/6 mice. In some experiments, we used B10 cell donor mice that had survived for 30–45 days after tumor challenge (10^5 BL3750 cells on day 0) and CD20 mAb treatment (250 μg on day 1). Similar results were obtained when the donor B cells were isolated from naive mice or mice that had survived BL3750 challenge, so all results were pooled.

TLR transcript expression. Total RNA was isolated from whole spleen cells, splenic B cells purified using B220-mAb coated microbeads, and BL3750 cells using TRIzol reagent (Invitrogen). Random hexamer primers (Promega) and Superscript II RNase H Reverse Transcriptase (Invitrogen) were used to generate cDNA. PCR primer pairs were used to amplify TLR transcripts as described (70). Relative TLR transcript levels were also quantified by GeneChip analysis (Affymetrix). Chip transcript levels were normalized to the 50th percentile using GeneSpring software (Agilent Technologies).

Cell proliferation and IL-10 secretion. Purified splenic B cells or BL3750 cells were labeled with CFSE Vybrant CFDA SE Fluorescent Dye (5 μM; Invitrogen). Labeled B cells were then cultured in medium with LPS (25 μg/ml), CpG (25 μg/ml), poly(I:C) (25 μg/ml), or recombinant mouse IL-10 (10 ng/ml; Biolegend) for 72 hours, with cell division assessed by

flow cytometry. For IL-10 measurements, purified B cells or BL3750 cells (4×10^5) were cultured in 0.2 ml of complete medium with TLR agonists in 96-well flat-bottom tissue culture plates. Culture supernatant fluid IL-10 concentrations were quantified using IL-10 OptEIA ELISA kits (BD Biosciences — Pharmingen) following the manufacturer's protocols. All assays were carried out using triplicate samples.

In vitro monocyte assays. Mouse splenic CD1d^{hi}CD5$^+$ or CD1d^{lo}CD5$^-$ B cells were purified by cell sorting and cultured with LPS (10 μg/ml) for 24 hours. Bone marrow CD11b$^+$ cells (1×10^6/ml) were purified using CD11b microbeads (Miltenyi Biotec) and cultured alone or with LPS-stimulated CD1d^{hi}CD5$^+$ or CD1d^{lo}CD5$^-$ B cells (1×10^6/ml) for 24 hours. Brefeldin A and LPS (1 μg/ml) were added during the final 4 hours of culture. Relative cytoplasmic TNF-α production by CD11b$^+$ cells was assessed by immunofluorescence staining. For TNF-α secretion, peritoneal macrophages from thioglycollate-treated mice were isolated by adherence to plastic with more than 85% purity, as determined by immunofluorescence F4/80$^+$ staining, and cultured alone or with LPS-stimulated CD1d^{hi}CD5$^+$ or CD1d^{lo}CD5$^-$ B cells (1×10^6/ml) for 48 hours, with LPS (1 μg/ml) added during the final 18 hours of culture. Tissue culture supernatant fluid TNF-α concentrations were quantified using TNF-α OptEIA ELISA kits (BD Biosciences — Pharmingen). To assess nitric oxide production, supernatant fluid was obtained from cells that were cocultured for 48 hours, with LPS (1 μg/ml) added during the final 18 hours of culture. Nitrite formed from the spontaneous oxidation of nitric oxide was quantified for duplicate samples using a Griess Reagent Kit (Invitrogen–Molecular Probes) following the manufacturer's protocols.

In vitro antibody-dependent phagocytosis assays. Spleen B cells were purified using a B cell isolation kit (Miltenyi Biotec), labeled with CFSE Vybrant CFDA SE Fluorescent Dye (5 μM), and cultured overnight in complete medium. CFSE-labeled B cells were incubated with MB20-11 CD20 mAbs on ice for 1 hour and then washed to remove unbound mAbs. Peritoneal macrophages from thioglycollate-treated mice were isolated by adherence to plastic and cultured for 18 hours with or without TLR agonists (10 or 25 μg/ml) added to the culture medium. Macrophages and B cells were mixed at a 1:1 ratio and cultured for 2.5 hours. The cells were then stained for cell-surface CD11b expression with CFSE$^+$CD11b$^+$ double-positive cell frequencies assessed by flow cytometry.

Statistics. Data represent mean ± SEM. Statistical comparisons of differences between sample means used the 2-tailed Student's *t* test. The generation of Kaplan-Meier cumulative survival plots and log-rank test comparisons of survival used Prism software (version 4.0; GraphPad Software). Cumulative survival differences were based on the survival days shown in each figure, even though some mice remained disease free. Spearman's rank correlation coefficient was used to determine the relationship between 2 variables. $P \leq 0.05$ was considered significant.

Study approval. The Duke University Animal Care and Use Committee approved all studies.

Acknowledgments

We thank Jacquelyn Bryant and David DiLillo, Karen Haas, and Jonathan Poe for help with this study and manuscript, and You-Wen He and Hanno Hock for providing mice. This work was supported by grants from the NIH (AI057157 and AI56363), La Fondation de France, and La Federation Nationale des Centres de Lutte Contre le Cancer (to V. Minard-Colin).

Received for publication May 31, 2011, and accepted in revised form September 21, 2011.

Address correspondence to: Thomas F. Tedder, Box 3010, Department of Immunology, Room 353 Jones Building, Research Drive, Duke University Medical Center, Durham, North Carolina 27710, USA. Phone: 919.684.3578; Fax: 919.684.8982; E-mail: thomas.tedder@duke.edu.

1. Anderson KC, Bates MP, Slaughenhoupt B, Pinkus G, Schlossman SF, Nadler LM. Expression of human B cell-associated antigens on leukemias and lymphomas: a model of human B cell differentiation. *Blood*. 1984;63(6):1424–1433.
2. Maloney DG, et al. IDEC-C2B8: results of a phase I multiple-dose trial in patients with relapsed non-Hodgkin's lymphoma. *J Clin Oncol*. 1997; 15(10):3266–3274.
3. Coiffier B. Rituximab therapy in malignant lymphoma. *Oncogene*. 2007;26(25):3603–3613.
4. Smith MR. Rituximab (monoclonal anti-CD20 antibody): mechanisms of action and resistance. *Oncogene*. 2003;22(47):7359–7368.
5. Hamaguchi Y, et al. The peritoneal cavity provides a protective niche for B1 and conventional B lymphocytes during anti-CD20 immunotherapy in mice. *J Immunol*. 2005;174(7):4389–4399.
6. McLaughlin P, et al. Rituximab chimeric anti-CD20 monoclonal antibody therapy for relapsed indolent lymphoma: half of patients respond to a four-dose treatment program. *J Clin Oncol*. 1998; 16(8):2825–2833.
7. Anolik JH, et al. The relationship of FcγRIIIa genotype to degree of B cell depletion by rituximab in the treatment of systemic lupus erythematosus. *Arthritis Rheum*. 2003;48(2):455–459.
8. Cartron G, et al. Therapeutic activity of humanized anti-CD20 monoclonal antibody and polymorphism in IgG Fc receptor FcγRIIIa gene. *Blood*. 2002; 99(3):754–758.
9. Weng W-K, Levy R. Two immunoglobulin G fragment C receptor polymorphisms independently predict response to rituximab in patients with follicular lymphoma. *J Clin Oncol*. 2003;21(21):3940–3947.
10. LeBien TW, Tedder TF. B-lymphocytes: How they develop and function. *Blood*. 2008;112(5):1570–1579.
11. Yanaba K, Bouaziz JD, Matsushita T, Magro CM, St Clair EW, Tedder TF. B-lymphocyte contributions to human autoimmune disease. *Immunol Rev*. 2008;223:284–299.
12. Mizoguchi A, Bhan AK. A case for regulatory B cells. *J Immunol*. 2006;176(2):705–710.
13. Bouaziz J-D, Yanaba K, Tedder TF. Regulatory B cells as inhibitors of immune responses and inflammation. *Immunol Rev*. 2008;224:201–214.
14. Mauri C, Ehrenstein MR. The 'short' history of regulatory B cells. *Trends Immunol*. 2008;29(1):34–40.
15. Fillatreau S, Gray D, Anderton SM. Not always the bad guys: B cells as regulators of autoimmune pathology. *Nat Rev Immunol*. 2008;8(5):391–397.
16. Rieger A, Bar-Or A. B-cell-derived interleukin-10 in autoimmune disease: regulating the regulators. *Nat Rev Immunol*. 2008;8(6):486–487.
17. Yanaba K, Bouaziz J-D, Haas KM, Poe JC, Fujimoto M, Tedder TF. A regulatory B cell subset with a unique CD1d^{hi}CD5$^+$ phenotype controls T cell-dependent inflammatory responses. *Immunity*. 2008;28(5):639–650.
18. Matsushita T, Yanaba K, Bouaziz J-D, Fujimoto M, Tedder TF. Regulatory B cells inhibit EAE initiation in mice while other B cells promote disease progression. *J Clin Invest*. 2008;118(10):3420–3430.
19. Moore KW, de Waal Malefyt R, Coffman RL, O'Garra A. Interleukin-10 and the interleukin-10 receptor. *Annu Rev Immunol*. 2001;19:683–765.
20. Iwata Y, et al. Characterization of a rare IL-10-competent B cell subset in humans that parallels mouse regulatory B10 cells. *Blood*. 2011;117(2):530–541.
21. Blair PA, et al. CD19$^+$CD24^{hi}CD38^{hi} B cells exhibit regulatory capacity in healthy individuals but are functionally impaired in systemic lupus erythematosus patients. *Immunity*. 2010;32(1):129–140.
22. Uchida J, et al. Mouse CD20 expression and function. *Int Immunol*. 2004;16(1):119–129.
23. Minard-Colin V, et al. Lymphoma depletion during CD20 immunotherapy in mice is mediated by macrophage FcγRI, FcγRIII, and FcγRIV. *Blood*. 2008;112(4):1205–1213.
24. Hamaguchi Y, Xiu Y, Komura K, Nimmerjahn F, Tedder TF. Antibody isotype-specific engagement of Fcγ receptors regulates B lymphocyte depletion during CD20 immunotherapy. *J Exp Med*. 2006; 203(3):743–753.
25. Uchida J, et al. The innate mononuclear phagocyte network depletes B lymphocytes through Fc receptor-dependent mechanisms during anti-CD20 antibody immunotherapy. *J Exp Med*. 2004; 199(12):1659–1669.
26. Hasegawa M, et al. B-lymphocyte depletion reduces skin fibrosis and autoimmunity in the tight-skin mouse model for systemic sclerosis. *Am J Pathol*. 2006;169(3):954–966.
27. Yanaba K, Hamaguchi Y, Venturi GM, Steeber DA, St. Clair EW, Tedder TF. B cell depletion delays collagen-induced arthritis in mice: arthritis induction requires synergy between humoral and cell-mediated immunity. *J Immunol*. 2007;179(2):1369–1380.
28. DiLillo DJ, et al. Maintenance of long-lived plasma cells and serological memory despite mature and memory B cell depletion during CD20 immunotherapy in mice. *J Immunol*. 2008;180(1):361–371.
29. Xiu Y, et al. B lymphocytes depletion by CD20 monoclonal antibody prevents diabetes in NOD mice despite isotype-specific differences in FcγR effector

functions. *J Immunol*. 2008;180(5):2863–2875.
30. Yanaba K, Bouaziz J-D, Matsushita T, Tsubata T, Tedder TF. The development and function of regulatory B cells expressing IL-10 (B10 cells) requires antigen receptor diversity and TLR signals. *J Immunol*. 2009;182(12):7459–7472.
31. Matsushita T, Tedder TF. Identifying regulatory B cells (B10 cells) that produce IL-10. *Methods Mol Biol*. 2010;677:99–111.
32. Dzhagalov I, St. John A, He YW. The antiapoptotic protein Mcl-1 is essential for the survival of neutrophils but not macrophages. *Blood*. 2007; 109(4):1620–1626.
33. Hock H, et al. Intrinsic requirement for zinc finger transcription factor Gfi-1 in neutrophil differentiation. *Immunity*. 2003;18(1):109–120.
34. Kawai T, Adachi O, Ogawa T, Takeda K, Akira S. Unresponsiveness of MyD88-deficient mice to endotoxin. *Immunity*. 1999;11(1):115–122.
35. Yazawa N, Hamaguchi Y, Poe JC, Tedder TF. Immunotherapy using unconjugated CD19 monoclonal antibodies in animal models for B lymphocyte malignancies and autoimmune disease. *Proc Natl Acad Sci USA*. 2005;102(42):15178–15183.
36. Tedder TF, Baras A, Xiu Y. Fcγ receptor-dependent effector mechanisms regulate CD19 and CD20 antibody immunotherapies for B lymphocyte malignancies and autoimmunity. *Springer Semin Immunopathol*. 2006;28(4):351–364.
37. Cittera E, et al. The CCL3 family of chemokines and innate immunity cooperate in vivo in the eradication of an established lymphoma xenograft by rituximab. *J Immunol*. 2007;178(10):6616–6623.
38. Heinz S, et al. Species-specific regulation of toll-like receptor 3 genes in men and mice. *J Biol Chem*. 2003;278(24):21502–21509.
39. Gururajan M, Jacob J, Pulendran B. Toll-like receptor expression and responsiveness of distinct murine splenic and mucosal B-cell subsets. *PLoS One*. 2007;2(9):e863.
40. Barr TA, Brown S, Ryan G, Zhao J, Gray D. TLR-mediated stimulation of APC: Distinct cytokine responses of B cells and dendritic cells. *Eur J Immunol*. 2007;37(11):3040–3053.
41. Schröder M, Bowie AG. TLR3 in antiviral immunity: key player or bystander? *Trends Immunol*. 2005; 26(9):462–468.
42. Stebbing N, Grantham CA. Anti-viral activity against encephalomyocarditis virus and Semliki Forest virus and acute toxicity of poly I and poly C administered sequentially to mice. *Arch Virol*. 1976;51(3):199–215.
43. Robinson RA, DeVita VT, Levy HB, Baron S, Hubbard SP, Levine AS. A phase I-II trial of multiple-dose polyriboinosic-polyribocytidylic acid in patients with leukemia or solid tumors. *J Natl Cancer Inst*. 1976;57(3):599–602.
44. Levy HB, et al. A modified polyriboinosinic-polyribocytidylic acid complex that induces interferon in primates. *J Infect Dis*. 1975;132(4):434–439.
45. Hendrix CW, et al. Biologic effects after a single dose of poly(I):poly(C_{12}U) in healthy volunteers. *Antimicrob Agents Chemother*. 1993;37(3):429–435.
46. Thompson KA, et al. Results of a double-blind placebo-controlled study of the double-stranded RNA drug polyI:polyC_{12}U in the treatment of HIV infection. *Eur J Clin Microbiol Infect Dis*. 1996;15(7):580–587.
47. Ambrus JL Sr, Chadha KC, Islam A, Akhter S, Ambrus JL Jr. Treatment of viral and neoplastic diseases with double-stranded RNA derivatives and other new agents. *Exp Biol Med (Maywood)*. 2006; 231(8):1283–1286.
48. Giantonio BJ, et al. Toxicity and response evaluation of the interferon inducer poly ICLC administered at low dose in advanced renal carcinoma and relapsed or refractory lymphoma: a report of two clinical trials of the Eastern Cooperative Oncology Group. *Invest New Drugs*. 2001;19(1):89–92.
49. Gowen BB, et al. TLR3 is essential for the induction of protective immunity against Punta Toro Virus infection by the double-stranded RNA (dsRNA), poly(I:C_{12}U), but not poly(I:C): differential recognition of synthetic dsRNA molecules. *J Immunol*. 2007;178(8):5200–5208.
50. Nicodemus CF, Wang L, Lucas J, Varghese B, Berek JS. Toll-like receptor–3 as a target to enhance bioactivity of cancer immunotherapy. *Am J Obstet Gynecol*. 2010;202(1):608.
51. Byrd JC, et al. Rituximab using a thrice weekly dosing schedule in B-cell chronic lymphocytic leukemia and small lymphocytic lymphoma demonstrates clinical activity and acceptable toxicity. *J Clin Oncol*. 2001;19(8):2153–2164.
52. O'Brien SM, et al. Rituximab dose-escalation trial in chronic lymphocytic leukemia. *J Clin Oncol*. 2001; 19(8):2165–2170.
53. Wooldridge JE, Ballas Z, Krieg AM, Weiner GJ. Immunostimulatory oligodeoxynucleotides containing CpG motifs enhance the efficacy of monoclonal antibody therapy of lymphoma. *Blood*. 1997; 89(8):2994–2998.
54. van Ojik HH, et al. CpG-A and B oligodeoxynucleotides enhance the efficacy of antibody therapy by activating different effector cell populations. *Cancer Res*. 2003;63(17):5595–5600.
55. Jahrsdorfer B, et al. CpG DNA increases primary malignant B cell expression of costimulatory molecules and target antigens. *J Leukoc Biol*. 2001; 69(1):81–88.
56. Friedberg JW, et al. Combination immunotherapy with a CpG oligonucleotide (1018 ISS) and rituximab in patients with non-Hodgkin lymphoma: increased interferon-α/β-inducible gene expression, without significant toxicity. *Blood*. 2005; 105(2):489–495.
57. Leonard JP, et al. Phase I trial of toll-like receptor 9 agonist PF-3512676 with and following rituximab in patients with recurrent indolent and aggressive non Hodgkin's lymphoma. *Clin Cancer Res*. 2007;13(20):6168–6174.
58. Huang B, Zhao J, Unkeless JC, Feng ZH, Xiong H. TLR signaling by tumor and immune cells: a double-edged sword. *Oncogene*. 2008;27(2):218–224.
59. Heikenwalder M, et al. Lymphoid follicle destruction and immunosuppression after repeated CpG oligodeoxynucleotide administration. *Nat Med*. 2004;10(2):187–192.
60. James SE, et al. Antibody-mediated B cell depletion before adoptive immunotherapy with T cells expressing CD20-specific chimeric T cell receptors facilitates eradication of leukemia in immunocompetent mice. *Blood*. 2009;114(27):5454–5463.
61. Matsushita T, Horikawa M, Iwata Y, Tedder TF. Regulatory B cells (B10 cells) and regulatory T cells have independent roles in controlling EAE initiation and late-phase immunopathogenesis. *J Immunol*. 2010;185(4):2240–2252.
62. Poe JC, et al. Amplified B lymphocyte CD40 signaling drives regulatory B10 cell expansion in mice. *PLoS One*. 2011;6(7):e22464.
63. Qin Z, Richter G, Schuler T, Ibe S, Cao X, Blankenstein T. B cells inhibit induction of T cell-dependent tumor immunity. *Nat Med*. 1998;4(5):627–630.
64. Shah S, et al. Increased rejection of primary tumors in mice lacking B cells: inhibition of anti-tumor CTL and TH1 cytokine responses by B cells. *Int J Cancer*. 2005;117(4):574–586.
65. Inoue S, Leitner WW, Golding B, Scott D. Inhibitory effects of B cells on antitumor immunity. *Cancer Res*. 2006;66(15):7741–7747.
66. Adachi O, et al. Targeted disruption of the MyD88 gene results in loss of IL-1- and IL-18-mediated function. *Immunity*. 1998;9(1):143–150.
67. Poe JC, et al. CD22 regulates B lymphocyte function in vivo through both ligand-dependent and ligand-independent mechanisms. *Nat Immunol*. 2004;5(10):1078–1087.
68. Sato S, Ono N, Steeber DA, Pisetsky DS, Tedder TF. CD19 regulates B lymphocyte signaling thresholds critical for the development of B-1 lineage cells and autoimmunity. *J Immunol*. 1996;157(10):4371–4378.
69. Van Rooijen N, Sanders A. Liposome mediated depletion of macrophages: mechanism of action, preparation of liposomes and applications. *J Immunol Methods*. 1994;174(1–2):83–93.
70. Edwards AD, et al. Toll-like receptor expression in murine DC subsets: lack of TLR7 expression by CD8α$^+$ DC correlates with unresponsiveness to imidazoquinolines. *Eur J Immunol*. 2003;33(4):827–833.